3-D Numerical Field Calculations of Magnets

Z. Greenwald, S. Greenwald
Laboratory of Nuclear Studies, Cornell University, Ithaca, NY 14853

Introduction

The 3-D numerical code BST.c described in CON 96-09 has subroutines which calculate the spatial magnetic fields generated by a wire carrying current. In particular,it calculates fields of wire loops wrapped on a pipe. The arrangement and dimensions of the loops can be easily modified to create dipoles, quadrupoles, skew magnets etc.. An example is the no-iron super conducting quadrupole dipole combination designed for CESR phase III upgrade (which will be manufactured by TESLA). The code is also used to calculate local fields errors due to possible manufacturing imperfections. An example of a rotational error of one pole, and an example of an error in the winding width are shown.

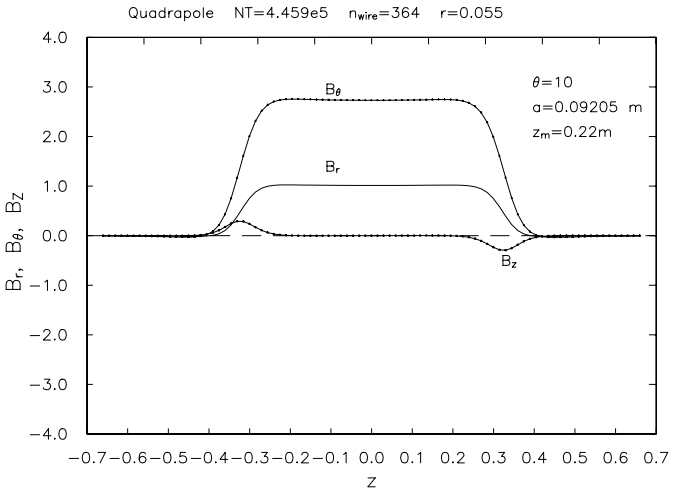

Figure 1: Quadrupole Magnetic Fields - 14 layers with elliptical loops at each pole ends. The perimeter of each layer is kept constant

1 *Quadrupoles*

An example of the magnetic fields of a quadrupole made out of four loops of wire ribbon is shown in Figure 1. The ribbon loops are wrapped on the pipe touching each other and creating four poles. (Current flows in opposite direction in each loop). The arcs of the loops are elliptical and all the layers have the same perimeter. Note, the field in the z direction B_z at the arcs is not zero. This field causes a higher order multipole. To suppress this field, each loop is divided into three sub concentric loops. See figure 2 for the $TESLA$ suggested structure and Figure 3 for the corresponding fields. In this configuration the field in the z direction B_z at the ends is spread and the peak field was reduced by 35 % (at $\theta = 10°$). Since the superconducting magnet for phase III will be installed inside CLEO, it is important to know the fields values outside the magnet. These fields are not small because the magnet does not have iron. Figure 4 shows that the magnetic fields B_r, B_θ at $r = 0.16m$, $\theta = 20.47°$ are of the order of 1. $Tesla$. (the quadrupole inner radius is $a = 0.09205\ m$). The magnetic fields as function of the azimuthal angle θ and the radius r at the end of the magnet $z = 0.033\ m$ are shown in Figure 5 and Figure 6 correspondingly.

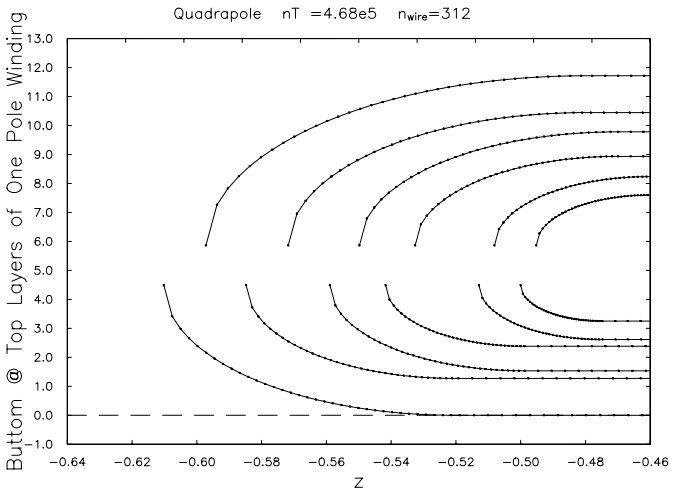

Figure 2: TESLA's suggested Quadrupole 14 layers with three elliptical loops at each pole end. The perimeter of each layer is kept constant

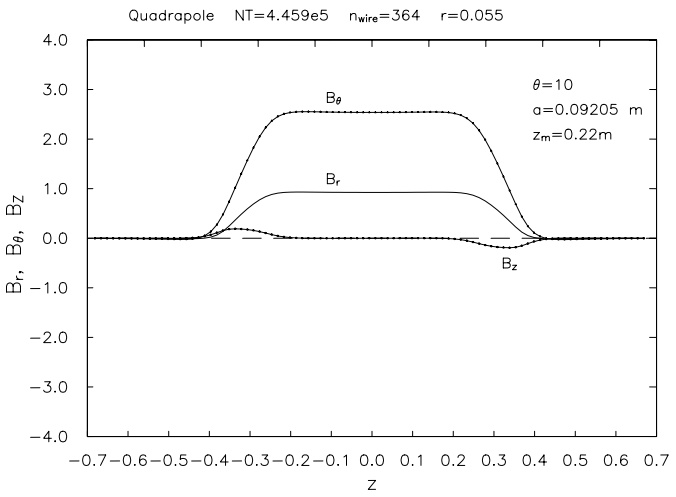

Figure 3: Magnetic Field of the TESLA Quadrupole with the ends shown in Figure 2 for $r < a$

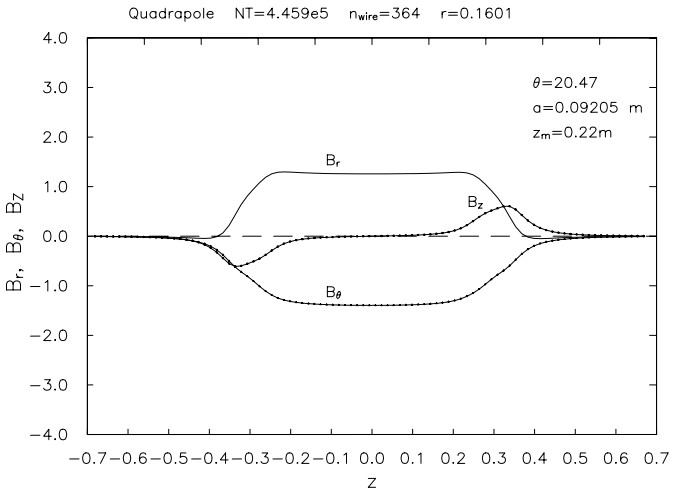

Figure 4: Magnetic Field of the TESLA Quadrupole with the ends shown in Figure 2 for $r > a$

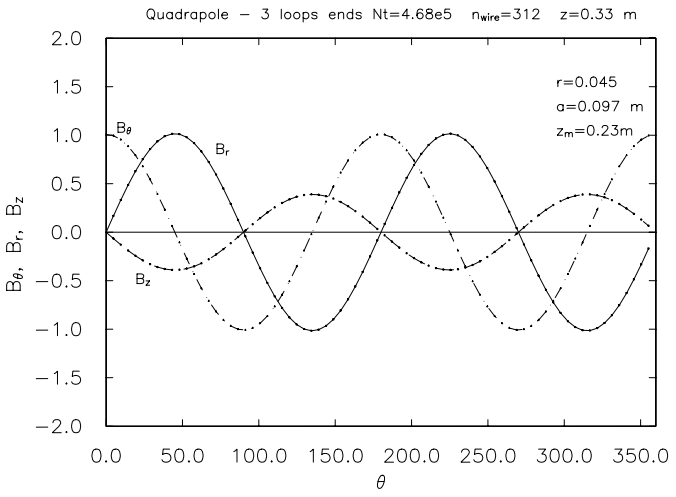

Figure 5: Magnetic Field of the TESLA Quadrupole along θ

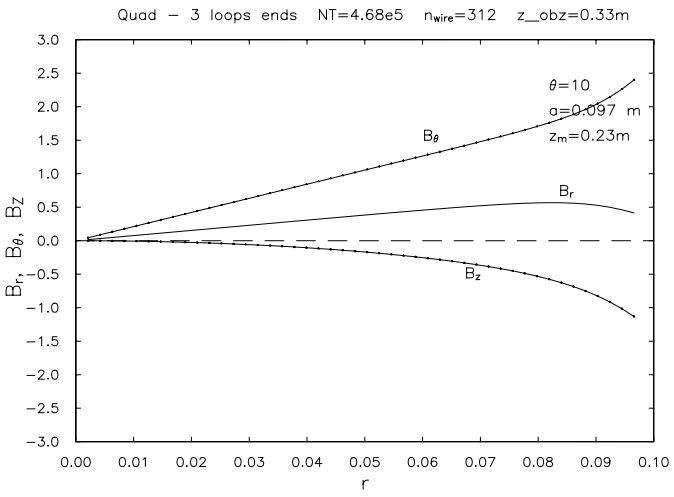

Figure 6: Magnetic Field of the TESLA Quadrupole along r

2 *Dipole*

Because of space limitation and cryogenic cooling, the dipole in phase III may be wound up on top of the quadrupole. Its length is bounded by the inner length of the quadrupole. These considerations make the dipole loops a complete ellipse (with only 7.9 mm of a straight line). The calculated field inside ($r < 0.14\ m$) and outside the magnet for this dipole are seen in Figures 7-11.

3 *Quadrupoles and Dipole combined*

The combined field of the quadrupole and dipole together are seen in Figure 12 for $r < a$ and Figure 13 $r > a$. The quadrupole fields are distorted by the added dipole winding as can be seen by comparing with the quadrupole fields (Figures 4,5).

4 *Winding Errors*

Possible displacement of the magnet wires during winding can cause errors in the magnetic fields. Two such examples are calculated. In the first case the center of one loop of the quadrupole is shifted by 1^o. In the second case the width of two poles of the quadrupole are smaller by 2. %. The errors in the field along θ relative to a perfect winding are shown in Figures 14 and Figure 15 correspondingly. In these examples the local fields distortion were of the order of $4 - 5\%$.

Acknowledgment

We would like to thank Gerry Dugan for very helpful discussions.

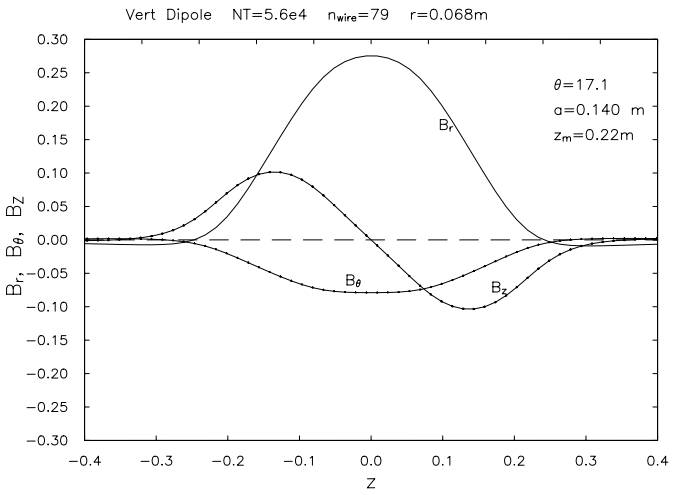

Figure 7: Dipole Magnetic Field along the z direction at $r = 0.068\ m$

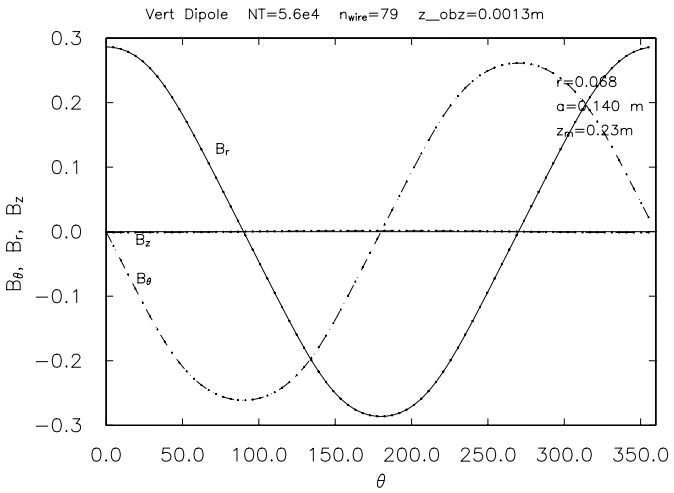

Figure 8: Dipole Field Inside the Pipe $r = 0.068\ m$ at the Center of the magnet

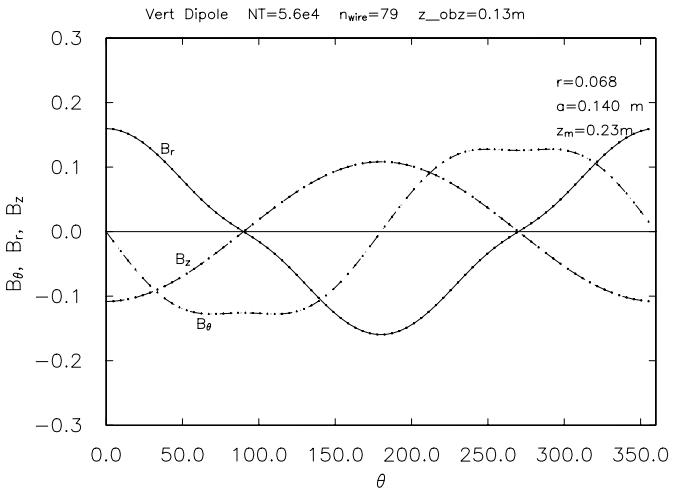

Figure 9: Dipole Field Inside the Pipe at $r = 0.068\ m$ at the End of the magnet

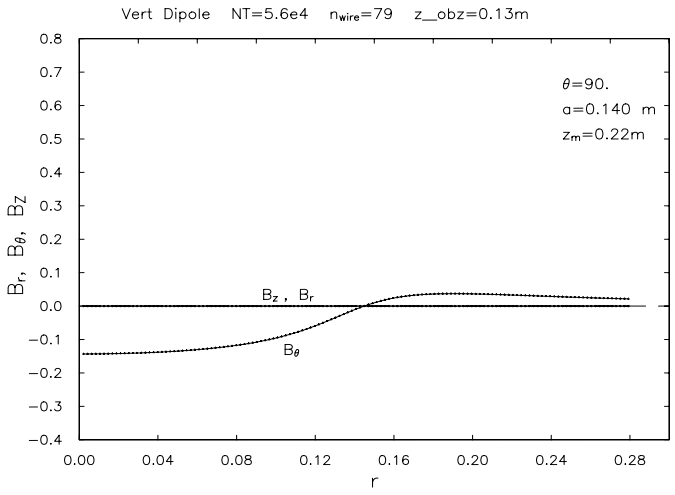

Figure 10: Dipole Field along r for $\theta = 90.^\circ$ at the End of the magnet.

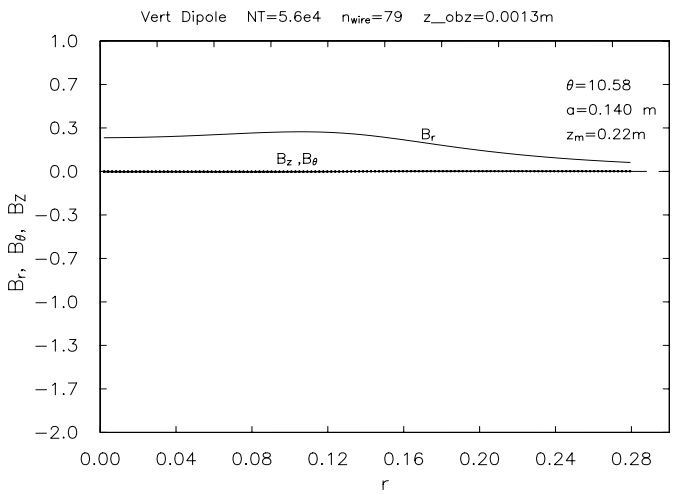

Figure 11: Dipole Field along r for $\theta = 0.^\circ$ at the center of the magnet.

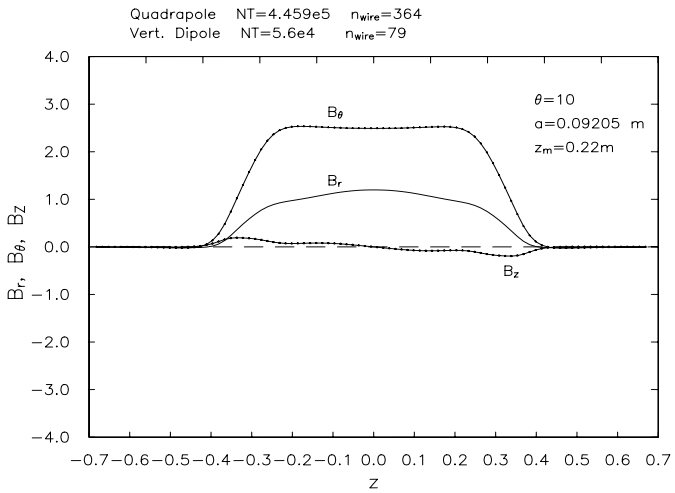

Figure 12: Combined Field of the above Quadrupole and Dipole at $r = 0.055\ m$ at $z = 0.13\ m$.

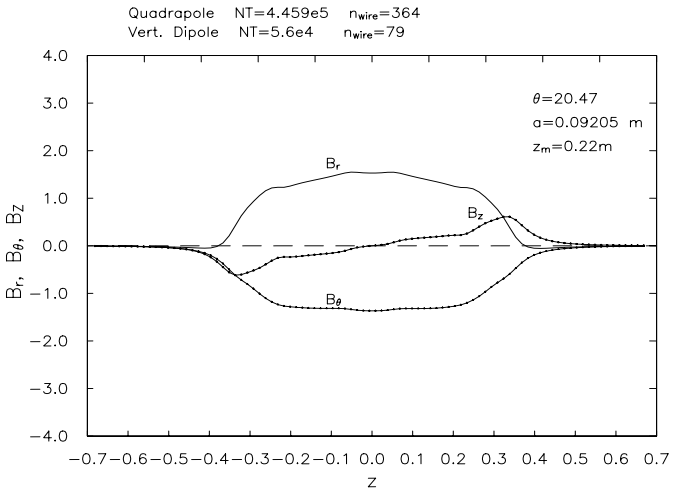

Figure 13: Combined Field of the above Quadrupole and Dipole at $r = 0.1601\ m$ at $z = 0.13\ m$.

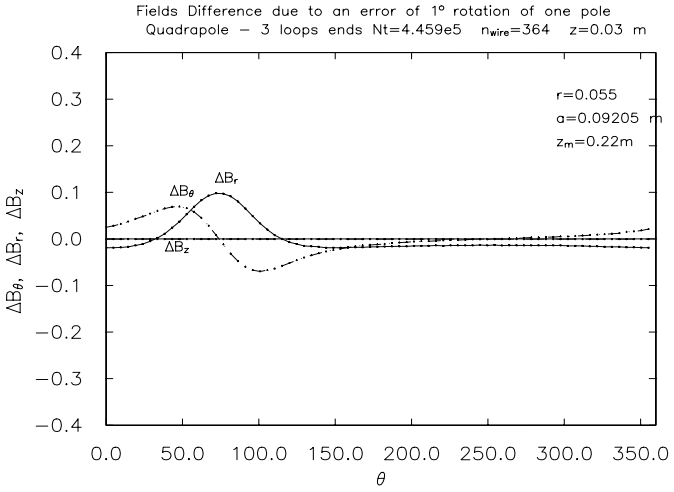

Figure 14: Field errors due to 1° shift in the center of one loop

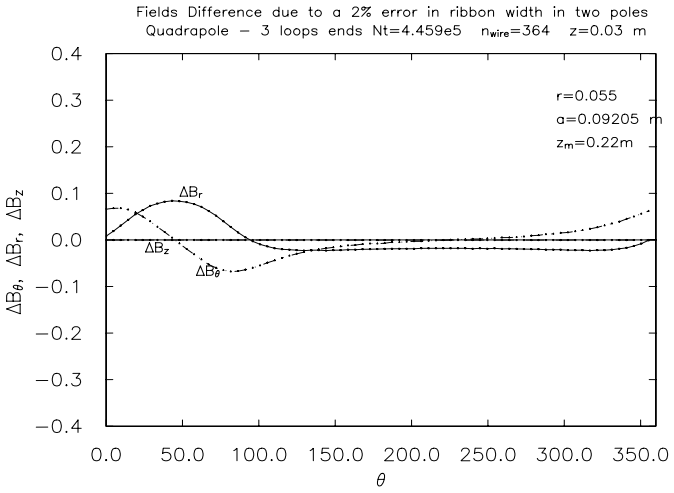

Figure 15: Fields error due to a 2 % decrease in the width of two poles